Simulation study to improve the detection of planar defects located under shrinkage cavities

Souad BANNOUF[1], Sébastien LONNE[1], Fabrice FOUCHER[1],
Jérôme DELEMONTEZ[2], Laetitia CHAPPAZ[2]

[1] EXTENDE, 15 Avenue Emile Baudot, Le Bergson, 91300 Massy, France, Fax +33 (0)9 72 13 42 68, e-mail : souad.bannouf@extende.com, sebastien.lonne@extende.com, fabrice.foucher@extende.com, www.extende.com
[2] EDF-Division Technique Générale, 21 AVENUE DE L'EUROPE, 38040 GRENOBLE, e-mail : jerome.delemontez@edf.fr, laetitia.chappaz@edf.fr

Abstract
This paper describes the study carried out by EXTENDE and the General Technical Division of EDF on the detection of defects located in a cast steel component including shrinkage cavities. Such casting defects appear within the material during solidification. Experimental measurements and simulations performed with CIVA showed that the presence of such cavities, especially when positioned at mid-thickness of the component, can mask planar type defects located at the bottom of the part and therefore prevent their potential detection. While conventional inspection with single element probe does not ensure breaking backwall notches detection, this can be achieved with phased array technology, provided that Signal to Noise Ratio is sufficient. Phased arrays, thanks to their deflection and focusing capabilities, limit the negative impact of shadowing but also allow to obtain high resolution images as the ones resulting from the Total Focusing Method (TFM). This innovative imaging technique proved its efficiency in detecting all the defects in the component while improving defect's provenance.

Keywords UT inspection, Cast Steels, shrinkage cavities, Simulation, Phased-array, Total Focusing Method (TFM)

1. Introduction

Conventional hydraulic and thermal production plants of EDF contain many ferritic cast steel parts which are subject to high stresses and constraints due to water pressure and damage by corrosion or thermal fatigue (see example in Figure 1). These parts are mainly inspected by surface testing performed from the inside because conventional ultrasonic controls reveal defects likely present since manufacturing. These flaws are considered non-progressive and harmless when they are not open to atmosphere. Most of the time, they consist in internal porosities as shrinkage cavities (typical manufacturing defects appearing during solidification of cast steel parts). The presence of these porosities - often present as clusters - can mask planar type defects located at the bottom of the part and therefore prevent their potential detection. In this context, the General Technical Division of EDF is studying the feasibility of an ultrasonic control, performed from the outer wall, of backwall breaking planar defects located beneath a shrinkage cavities network. Thus, EXTENDE has evaluated by simulation the feasibility of such an examination. Various methods have been studied: from conventional single-element inspection to phased array technology, through the evaluation of innovative techniques such as the Total Focusing Method (TFM). This paper describes the results obtained with the CIVA simulation software.

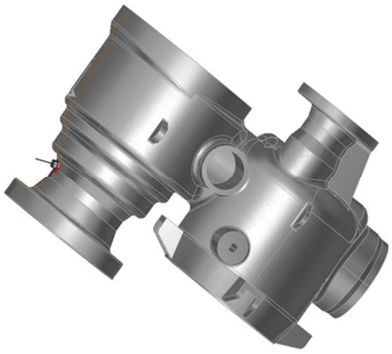

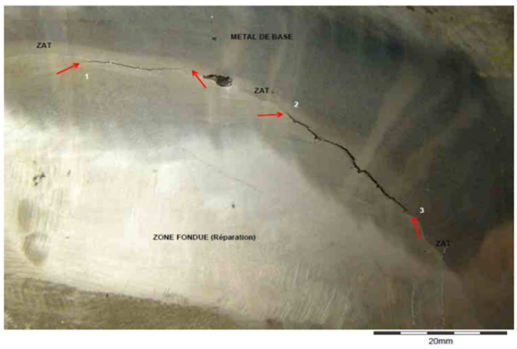

Figure 1 : Example of a cast steel part from a conventional thermal plant – example of creep damage found in inner wall.

2. Inspected component and flaws to detect

2.1 Specimen

The specimen to be inspected is, for simplicity purpose, a perfect portion of cylinder with dimensions equal to 285x100x70mm and 1400mm internal radius. The considered material is isotropic ferritic steel where noise and attenuation are neglected. Its characteristics are:

- Density: 7.8g.cm^{-3}
- Speed longitudinal waves: 5900m.s^{-1}
- Speed shear waves: 3230m.s^{-1}

The main objective of the work carried out by EXTENDE is to study the feasibility of an ultrasonic inspection of a notch located below a network of cavities. Therefore, simplifications in terms of geometry and material are justifiable.

2.2 Flaws

The considered flaw is a backwall breaking notch of dimensions 40x10mm (L×h). To study different scenarios (few shadowing, shadowing by one, two or three cavities), the notch is positioned at four positions relatively to the shrinkage cavities cluster. The porosities are defined by tracing their contour at -6dB from echoes recorded on an acquisition performed at EDF-DTG with a 1D smart flexible 2 MHz phased array probe used in manual mode (see Figure 2). The contours were then extruded on 20mm in the plane perpendicular to the incidence plane; the cavities are assumed to be constant in this plan.

Thus, seven (7) shrinkage cavities are defined and positioned at mid-thickness of the sample as shown on Figure 3. An eighth porosity is also placed at the bottom part to study the influence of interactions between casting defects potentially present in the vicinity of the inner wall and the target flaw.

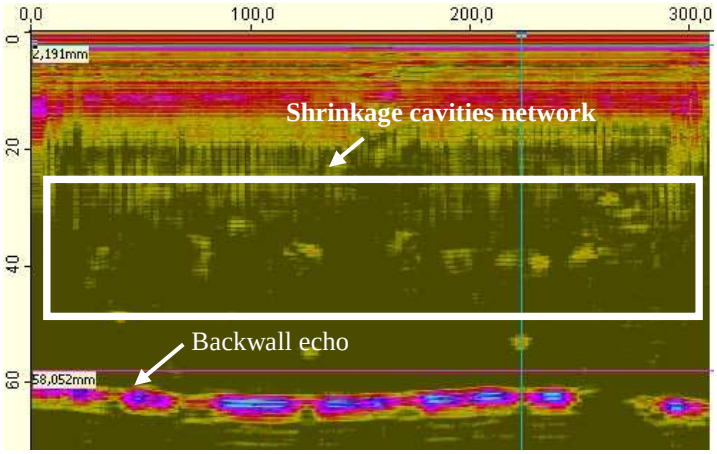

Figure 2 : Bscan showing the presence of shrinkage cavities in a cast steel specimen. The Bscan has been used to draw the porosities.

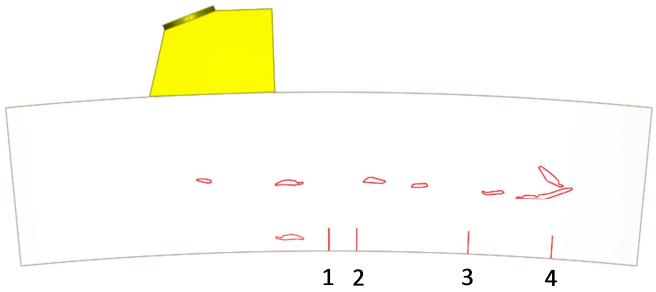

Figure 3 : Target notch positions relative to the shrinkage cavities network.

3. Evaluation of a single element ultrasonic conventional control

The backwall breaking notches located under the network of shrinkage cavities positioned at mid-thickness of the sample were inspected with a conventional OL45° single element probe of 2MHz and Ø24mm diameter.
Amplitudes are calibrated with the one of a Ø2mm Side Drilled Hole (SDH) located at 70mm from the surface and detected with the same probe.

Figures 4 and 5 show simulated Bscans for the notch when located at position 1 and 2 under the porosities cluster. For each position, the Bscan simulated with the notch is compared with the one simulated without notch in order to be sure that the echo on the Bscan belongs to the notch and not to a porosity.
Figure 4 presents the results when the flaw is at position 1. The comparison of Bscans with and without notch allows to confirm that the notch is well detected with a corner echo amplitude of 0.1 dB relatively to the SDH.

Despite the shrinkage cavities network, there is no problem for detecting the notch at position 1 which is not the case at position 2.

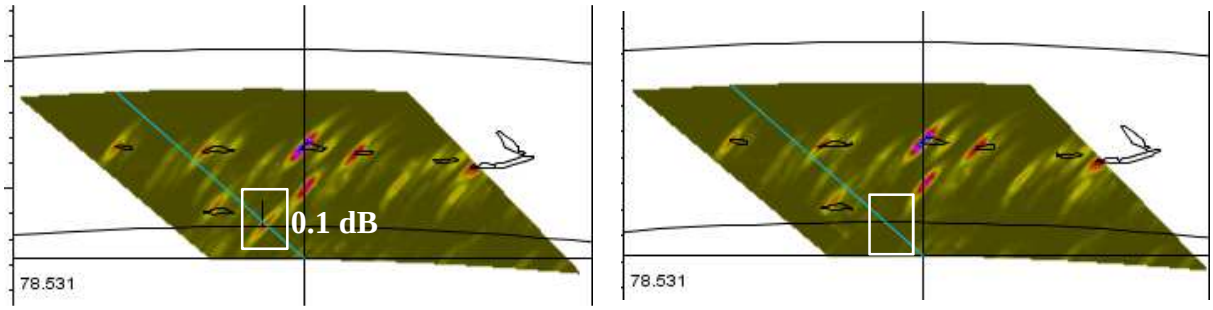

(a) (b)

Figure 4 : OL45° detection of the notch at position 1. (a) Bscan with notch, (b) Bscan without notch

Figure 5 shows simulated Bscans with and without the notch for position 2. It can be seen the corner echo is not exactly where it is expected to be. Furthermore, it has very low amplitude (-14 dB). Weak detection and bad positioning of the corner echo are due to the shrinkage cavities which mask the notch and deflect the acoustic beam.

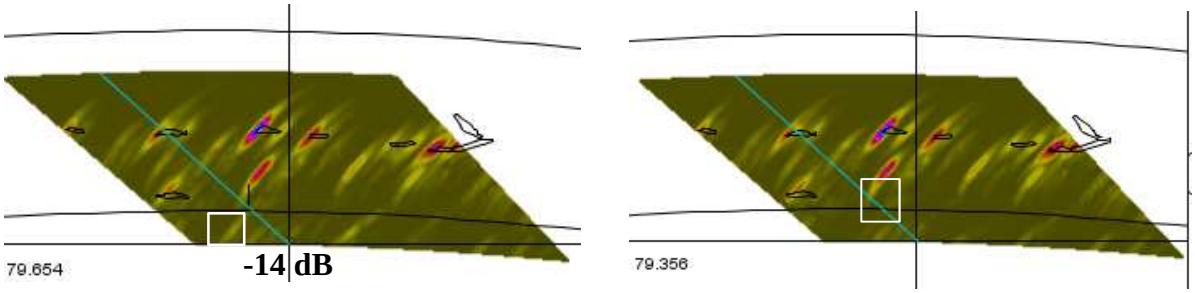

(a) (b)

Figure 5 : OL45° detection of the notch at position 2. (a) Bscan with notch, (b) Bscan without notch

The simulation results show that inspection with an OL45° single element probe cannot ensure notch detection for all positions under the shrinkage cavities network. The porosities located at mid-thickness can mask the notches which lower and/or prevent their detection.

4. Evaluation of the phased-array technology used in echographic mode

The simulation study with OL45° single element probe showed that it is not possible to ensure the notch detection for all positions under the cavities network. Therefore, phased-array technology has been evaluated under the same conditions in order to estimate its advantages relatively to conventional inspections.
The phased array probe used for simulation is a 2.25 MHz contact probe (48 elements, 0.8mm pitch) fixed on an OL45° Plexiglas wedge.

The amplitude of a Ø2mm SDH located at the notch depth and detected with a delay law focusing OL45° waves at 70mm depth. The simulated inspection consists in a mechanical scanning (0.05° step) associated with a sectorial scanning (from 0° to 60° with 2° step) focusing at 70mm depth.
Figures 6(a) and 7(a) show, respectively for position 1 and 2, sectorial Bscans where the notch corner echo is correctly detected. They are compared with simulations without notch in order to ease and confirm the echoes identification.
As presented on Figure 6, the notch echo can be identified. The inspection angle leading to its detection at position 1 is OL44° which is close to the angle used with the single element

probe. Therefore, at position 1, the shrinkage cavities network is not detrimental to the detection of the flaw when using approximately OL45° waves.

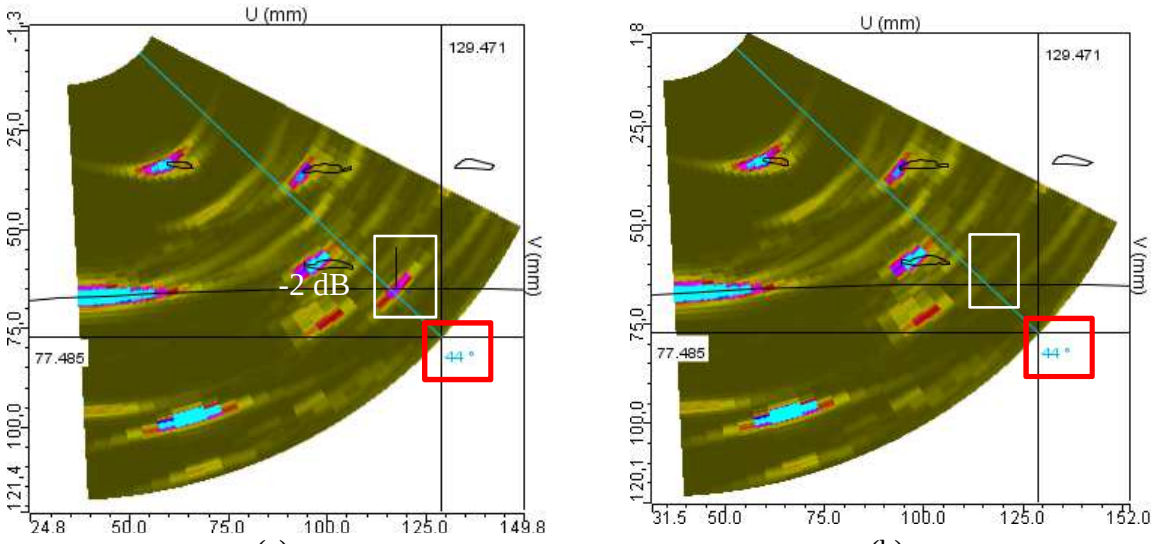

(a) (b)

Figure 6 : Angular Bscan at position n°1 : (a) with notch, (b) without notch

Simulated sectorial Bscans with and without the notch at position 2 are displayed on Figure 7. The comparison between simulated Bscans with and without the flaw confirms that the echo bordered in white belongs to the notch.

While inspection with OL45° single element probe does not lead to the clearly detection of the notch corner echo, inspection with focused sectorial scanning allows it. However, contrary to position 1, for the second position the suitable angle for the flaw unmasking is OL30°.

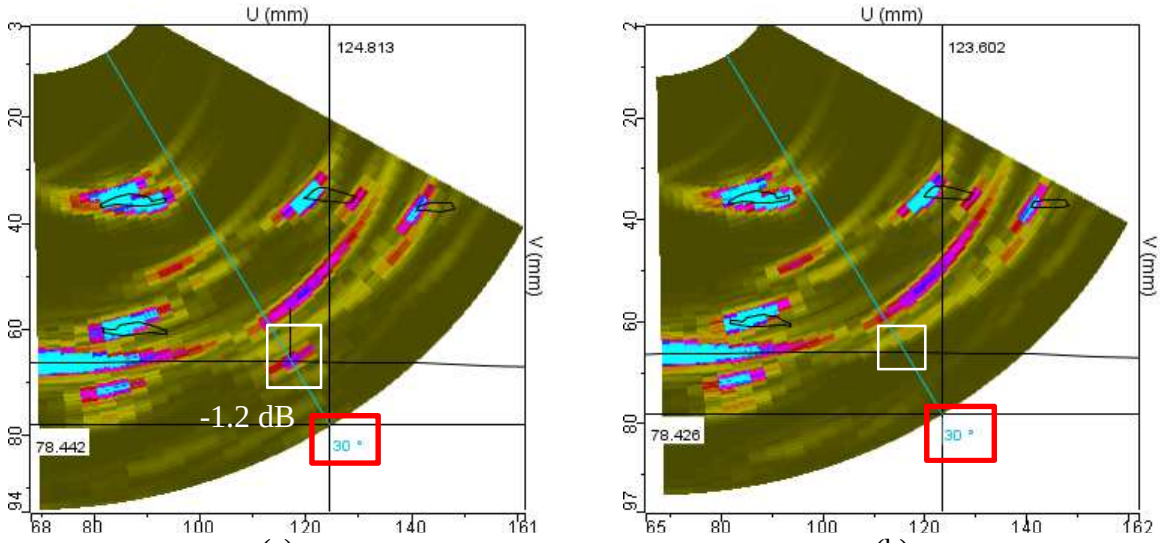

(a) (b)

Figure 7 : Angular Bscan at position n°2 : (a) with notch, (b) without notch

An OL30° inspection seems more adapted for the notch detection when it is located at position 2. Figure 8 (a) and (b) show the mechanical scanning True-Bscans obtained with phased-array technology when using OL30° and OL44° respectively. Their comparison highlights the importance of the inspection angle. At position 2, the notch location relatively

to the shrinkage cavities network is not favourable for an OL45° inspection because of the beam is stopped and/or deflected by the porosities and thus leading to poor results. This explains the bad results obtained with the single element probe transmitting OL45° waves.

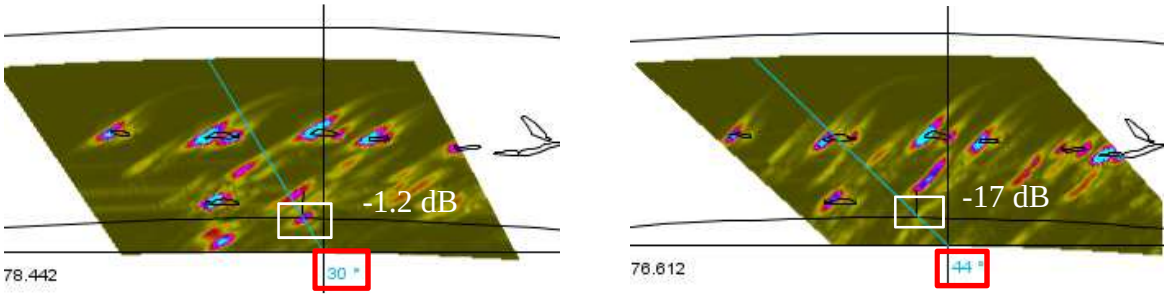

(a) (b)

Figure 8 : Comparison of OL30° and OL44° Bscans at position n°2: (a) OL30° Bscan, (b) OL44° Bscan

The results obtained with the phased array probe show that it is possible to detect the notch with the same transducer whatever its position under the shrinkage cavities network. Angular deflection limits the impact of the masking effect, the various angles of inspection maximize the notch detection according to its position relatively to the porosities cluster. Furthermore, the use of the phased-array technology increases resolution and positioning of the echoes in the CAD specimen by its focusing ability.

5. Contribution of the Total Focusing imaging Method

With the phased-array technology, the notch detection is ensured for all the studied positions but it is mainly restricted to the corner echo identification because the diffraction is too weak to be measured. In the presence of several porosities and structural noise, it may be difficult to determine the origin (cavity, notch, grain,…) of the echo supposed to be from the target flaw. Therefore, the Total Focusing Method (TFM) has been evaluated on its ability to improve flaw identification.

A FMC acquisition corresponds to a fixed array position acquisition of the full inter-element matrix **K**(*t*). For an array of N active elements, it is constituted by the N×N stored impulse inter-element responses $k_{ij}(t)$ defined as the output of the element number *j* when the input of the element number *i* is a delta impulse [1,2,3]. TFM is a synthetic imaging algorithm implemented in CIVA which post-processes the full inter-element matrix **K**(*t*) and provides a high resolution image of a Region Of Interest (ROI) [2,3]. Its principle is to coherently sum all elementary signals $k_{ij}(t)$ of **K**(*t*) in order to focus, *a posteriori*, in every point of the ROI. The amplitude A at the point M in the image is given by:

$$A(M) = \sum_{i,\,j} k_{ij}\left(T_{ij}^{M}\right) \qquad (1)$$

where T_{ij}^{M} is the theoretical time of flight between M and a pair of elements (*ij*).

In order to evaluate the advantages of TFM imaging on the notch detection, FMC acquisitions were performed at the positions ensuring the best results in echographic mode. Thus, the

detectability of the flaw according to the acquisition method (echographic or FMC-TFM) is tested.

Figures 9(b) and 10(b) correspond to the TFM notch reconstructions with LL direct mode. The direct mode is based on the calculation of theoretical times of flight corresponding to the propagation time between each pair of transmitter/receiver (*ij*) through a point M of the ROI. The comparison of TFM images with associated sectorial Bscan (Figure 9(a) and 10(a)) shows that the results are quite similar. The same echoes at the same positions are found on both FMC-TFM images and sectorial echographic Bscans.

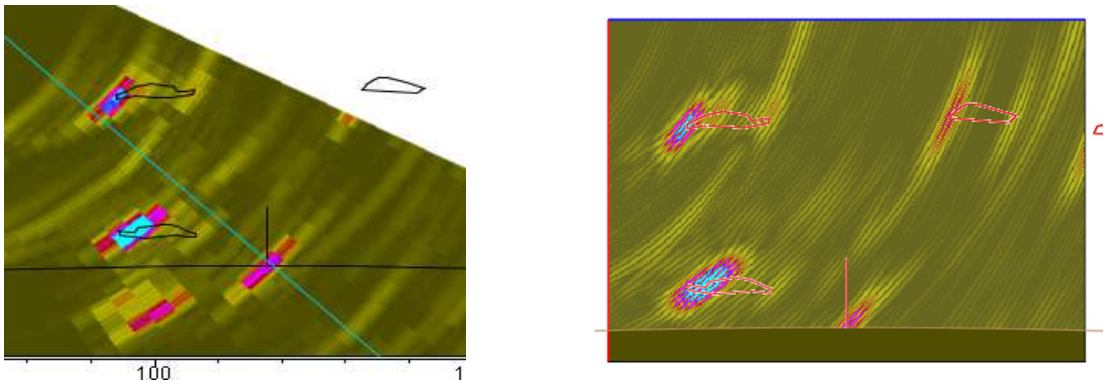

(a) (b)

Figure 9 : Images of the notch at position 1: (a) echographic mode, (b) LL direct mode TFM image

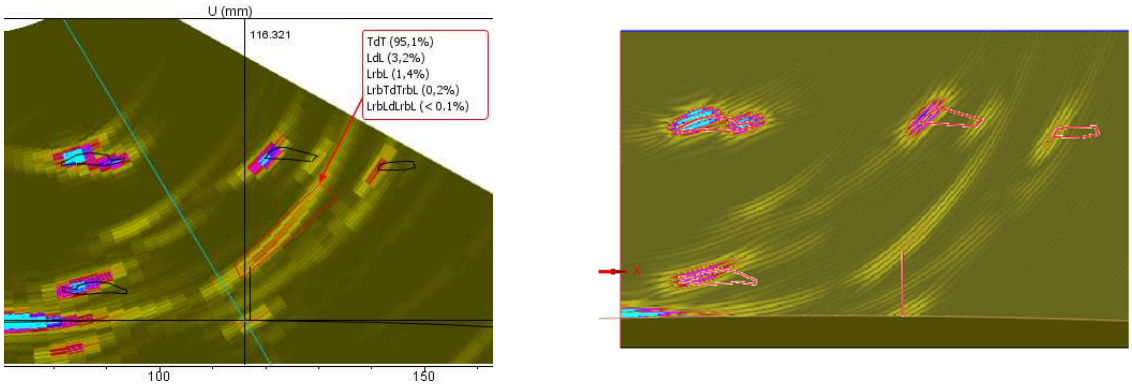

(a) (b)

Figure 10 : Images of the notch at position 2: (a) echographic mode, (b) LL direct mode TFM image

Besides providing high resolution images, the TFM imaging has another advantage compared to echographic imaging since it allows to image flaws according to paths more complex than the direct ones “probe/flaw”. This is possible thanks to the “corner echo” reconstruction. In the corner echo mode, the considered times of flight take into account the interaction of the wave and its possible mode conversions on the backwall before reaching the defect [2, 3, 4]. This mode is very useful for imaging extended defects such as notches.

A priori, it is not obvious to know the “corner echo mode” (among the 9 possible) that will image the notch, in the presence of the shrinkage cavities, along its entire length. However, the ray tracing tool of CIVA, although it does not take into account the elementary directivity of the emitted waves, can help finding an appropriate mode for reconstruction. Figure 11 shows the ray paths for position 1 and 2. For the first position, the ray tracing tool indicates

that a LLL path is possible. For position 2, a TTT path can be considered for the flaw imaging.

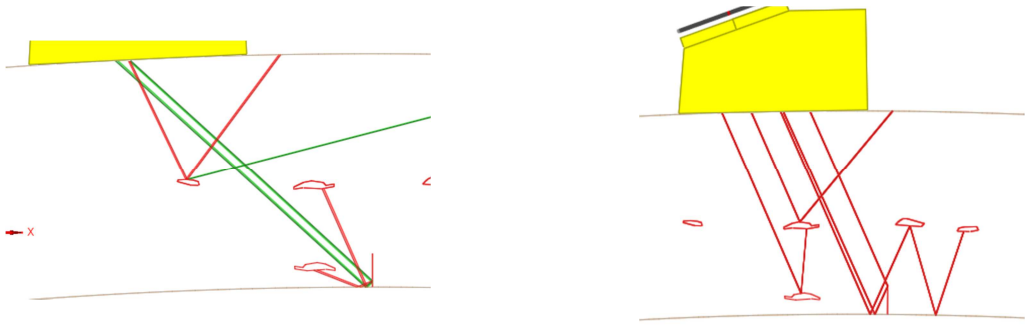

(a) (b)

Figure 11 : Ray tracing at 2 different probe positions: (a) position 1, (b) position 2

The paths on Figure 11, provided by the CIVA ray tracing tool, are used to obtain corner echo mode TFM images. The results are presented on Figure 12 for both studied positions.

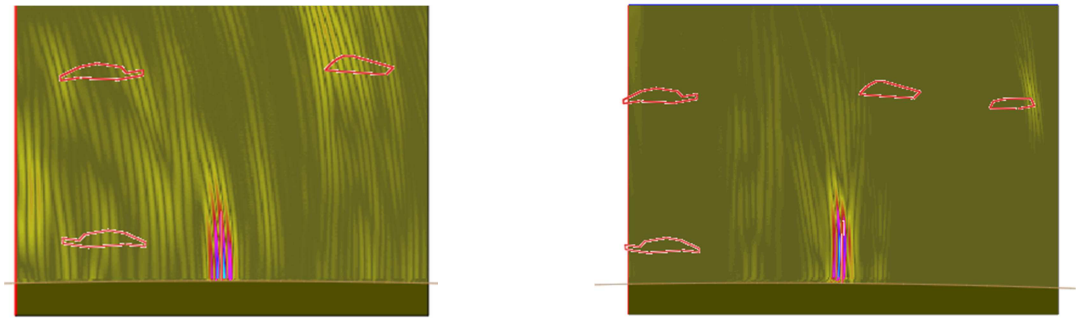

(a) (b)

Figure 12 : TFM Corner mode reconstruction images of the notch with :
(a) LLL mode - position 1, (b) TTT mode - position 2.

Whatever the notch position under the shrinkage cavities network, the corner mode reconstruction following the indications of the ray tracing tool allows to image the flaw on its entire length. Contrary to the direct mode, the notch is no more characterized by its two diffraction echoes.

Modes different from the ones provided by ray tracing were tested. As a result, only LLL and TTT modes lead in a correct reconstruction of the notch. However, when the probe is located near the planar defect, the dynamic of the notch in LLL mode is weaker than in TTT mode. It happens for position 2 where the probe center is located 30° from the notch. For this position, the LLL mode image shows, under the probe aperture, a strong artefact of reconstruction disturbing the image of the flaw (see Figure 13(a)).
The artefact corresponds to the backwall echo reconstruction with LLL mode. Indeed, in order to reproduce as precisely as possible the acoustic phenomena occurring in experiment, the backwall echo was calculated in simulation. The TFM algorithm searches for each pixel of the ROI the amplitude of the echoes – including the one from the backwall - located at a time of flight equivalent to a LLL path. Because a part of the ROI is located below the probe aperture,

the algorithm records information associated with the specimen backwall which creates the artefact. This one has the biggest dynamic on the image because the backwall echo has greater amplitude than the notch. In order to confirm the artefact origin, a simulation without backwall echo calculation was performed. The associated LLL mode image is shown on Figure 13(b). There is no more artefact, only the notch reconstructed along its entire length and with a better dynamic. Therefore, the specimen backwall echo causes the artefact in LLL mode. The artefact does not appear with TTT mode reconstruction since the times of flight searched by the algorithm to image the notch are far from the ones of the backwall.

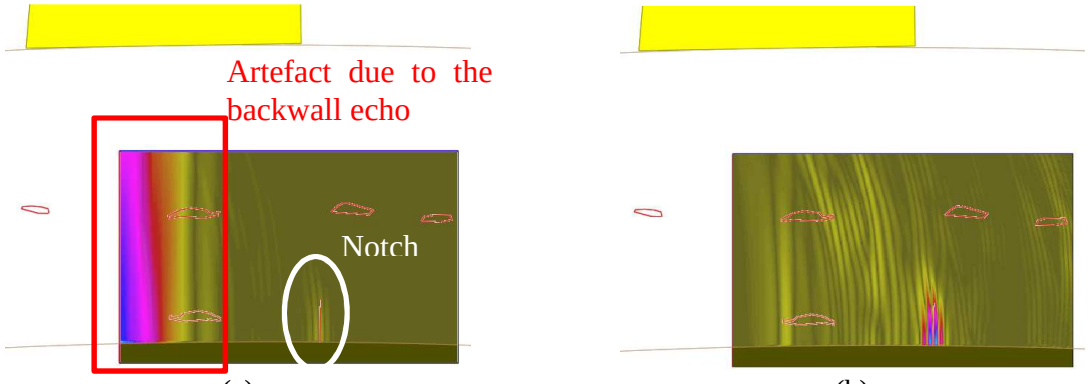

Figure 13 : TFM reconstruction of the notch with LLL corner (a) with backwall echo taken into account, (b) without backwall echo taken into account

In view of these results, it is possible to affirm that TFM imaging in LL mode provides as good results as standard sectorial echographic imaging. As for the corner mode, it improves the detection and identification of the flaw by imaging it along its entire length. Furthermore, it allows filtering from the image the strong cavities echoes present in echographic images or in LL mode reconstructions. Therefore, TFM is an imaging method that ensures the detection of a backwall breaking planar flaw despite the presence of a shrinkage cavities network disturbing the ultrasound waves path. It also allows to determine if the target echo observed in direct mode or echographic mode belongs to a porosity or a notch.

This conclusion remains valid provided there is a sufficient Signal to Noise Ratio (SNR). Indeed, with FMC acquisition, the firing with only one element at a time reduces the energy transmitted in the specimen. It may be non-impacting in low attenuating media but this may be more restrictive in noisy environments (SNR degradation, reduction of the detectability ...) such as coarse ferritic cast steels.

6. Conclusion

This paper describes a study carried out by EXTENDE and the General Technical Division of EDF on the detection of defects located in a cast steel component including shrinkage cavities. First, a conventional single-element OL45 ° inspection was considered. Simulations in CIVA showed that the presence of porosities can mask planar type defects located at the bottom of the specimen and thus potentially prevent their detection. The phased array technology was then used to evaluate its detection performances under the same conditions. Contrary to the conventional single-element inspection, the phased array probe allows the detection of the notch for all positions. This is an advantage because there is no need to

change the transducer since the delay laws can deflect the beam according various inspection angles and then ensure detection whatever the position of the notch relatively to the porosities. Therefore, deflection and focusing ability of a phased array probe help to control the negative effect of masking but it is not obvious to affirm without flawless simulation that the considered echo belongs to a notch since only the corner echo is identified. Because this one may be confused with a shrinkage cavity echo, the TFM method was evaluated on its ability to provide additional information about the origin of the echo of interest. Thus, the LL direct mode reconstruction allows to obtain images very similar to echographic ones, so it does not answer to the origin question. As for the corner echo reconstruction mode, it provides an image in which only appears the notch imaged along its entire length. This reconstruction method allows to identify unambiguously the presence of the flaw despite the shrinkage cavities network located on the ultrasonic waves path.
These results show that the detection of a breaking backwall notch below a network of porosities is possible. However, it is reminded that the structural noise was not modelled. Therefore, these results remain valid provided there is a sufficient SNR, especially for TFM imaging which FMC restricts the transmitted energy in the specimen. An experimental study is now necessary to validate these results.

References

1. C. Holmes, B. W. Drinkwater, Paul D. Wilcox, ‘Post-processing of the full matrix of ultrasonic transmit-receive array data for non-destructive evaluation’, NDT&E International, 38, 701-711 (2005)

2. S. Bannouf, ‘Développement et optimisation de méthodes d’imagerie synthétique pour le contrôle non-destructif par ultrasons de composants industriels complexes’, PhD thesis, Université Paris 7 Denis Diderot, 2013

3. S. Bannouf, S. Robert, O. Casula, C. Prada, ‘Evaluation of multi-element methods applied to complex geometries’, AIP Conf. Proc. 1430, 833, 2012

4. A. Fidahoussen, P. Calmon, M. Lambert, S. Paillard, S. Chatillon, ‘Imaging of Defects in Several Complex Configurations by Simulation-helped Processing of Ultrasonic Array Data’, Review of Quantitative Nondestructive Evaluation, Vol. 29, (2009), pp.847-854